Letters

A New-Variable-Coil-Structure-Based IPT System With Load-Independent Constant Output Current or Voltage for Charging Electric Bicycles

Yong Li, Jiefeng Hu, Feibin Chen, Shunpan Liu, Zhaotian Yan, and Zhengyou He

***Abstract*—This letter presents an inductive power transfer system based on a new variable coil structure to achieve load-independent constant current (CC) and constant voltage (CV) outputs for charging electric bicycles (EBs), without involving complex control strategies. The new variable coil structure consists of three-layer coils, i.e., two bipolar coils and one unipolar coil, on the transmitter side and one unipolar coil on the receiver side. The compact and portable receiver with series compensation is installed in the EB, while two switches on the transmitter side at the power charging station are utilized to reconfigure the transmitter coil structure to select the charging mode, i.e., CC mode or CV mode. The proposed system can achieve zero phase angle operation, fixed operating frequency, and zero-voltage switching, which will lower the power rating of power switches and improve the efficiency. A laboratory prototype is built to verify the feasibility of the proposed method.**

***Index Terms*—Constant current (CC), constant voltage (CV), electric bicycles (EBs), inductive power transfer (IPT).**

I. Introduction

ELECTRIC bicycles (EBs) play an important role in modern transportation due to their convenience and relatively long driving range [1]–[3]. The bicycle-sharing system and public bicycle transportation services are changing our lives. Traditionally, the battery is installed on the EB to store the electric energy, and the conventional plug-in charging system is widely used to charge EBs [4]. However, these charging systems feature low convenience and low safety. Besides, for security purpose in public-sharing EBs, instead of allowing users to take away the batteries, they are integrated into the EBs. Therefore, public charging stations using inductive power transfer (IPT) technology is an attractive solution to charge the EBs with its inherent advantages, e.g., safety, convenience, and reliability [3], [5].

Generally, the charging process for batteries consists of two main stages, i.e., constant current (CC) charging and constant voltage (CV) charging. During the entire charging process, the equivalent resistance of the battery significantly varies [3]. Therefore, it is challenging to design and control such a wireless charging system with CC and CV outputs for EBs with wide range various loads.

In the past few years, many approaches have been investigated to address the aforementioned issues. A simple solution is to utilize a dc–dc converter at the transmitter side or the receiver side to achieve the desired output current and voltage [6]. However, this approach will result in extra power losses and need extra space to install the bulky dc–dc converter. Regulating the operating frequency of the IPT system is another method is to realize the CV or CC output. However, it will lead to a stability issue, i.e., the frequency bifurcation phenomenon [7]. With specified operating frequencies, the series–series compensated IPT system with the load-independent CV output is proposed in [8]. However, the IPT system cannot guarantee zero phase angle (ZPA), which will increase the power rating of power switches and decrease the efficiency dramatically. Besides, the realization of the CC output in [8] is missing. In [9], hybrid topologies with the load-independent CC or CV output are realized by switching series compensation into parallel compensation on the transmitter side. However, it needs three switches and an extra inductor, which will increase the cost. In [3], a hybrid compensation topology on the receiver side is proposed to achieve the required CC or CV charging with a single inverter to charge multiple EBs simultaneously. However, additional components, i.e., an inductor, three capacitors, and two switches, are required on the receiver side, which will increase the weight and installation space of the EB.

To reduce the complexity and weight of the receiver that will be installed in the EB, a new variable coil structure, which consists of three-layer coils, i.e., two bipolar coils and one unipolar coil on the transmitter side and one-layer coil, i.e., unipolar coil on the receiver side, is proposed for the IPT system to charge EBs. The proposed IPT system can achieve load-independent

Manuscript received December 24, 2017; revised January 24, 2018; accepted March 2, 2018. Date of publication March 6, 2018; date of current version July 15, 2018. This work was supported in part by the National Key R&D Program of China (2017YFB1201002), in part by the Hong Kong Research Grant Council (PolyU 252040/17E), in part by Hong Kong Polytechnic University (1-ZE7J), and in part by the National Science Fund for Distinguished Young Scholars under Grant 51525702. *(Corresponding author: Zhengyou He.)*

Y. Li is with the Department of Electrical Engineering, Hong Kong Polytechnic University, Hung Hom, Hong Kong, and also with the School of Electrical Engineering, Southwest Jiaotong University, Chengdu 610031, China (e-mail: leeo1864@163.com).

J. Hu is with the Department of Electrical Engineering, Hong Kong Polytechnic University, Hung Hom, Hong Kong (e-mail: jerry.hu@polyu.edu.hk).

F. Chen, S. Liu, Z. Yan, and Z. He are with the School of Electrical Engineering, Southwest Jiaotong University, Chengdu 610031, China (e-mail: scsncfb@126.com; liusp@my.swjtu.edu.cn; zhaotian_Y@163.com; hezy@swjtu.cn).

Color versions of one or more of the figures in this letter are available online at http://ieeexplore.ieee.org.

Digital Object Identifier 10.1109/TPEL.2018.2812716

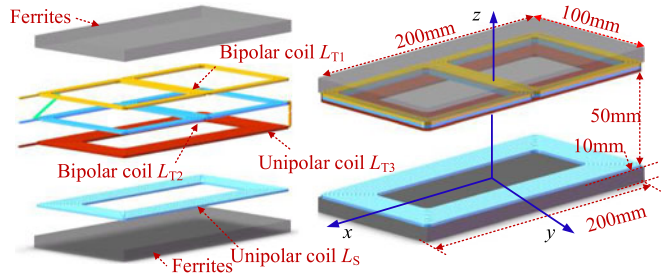

Fig. 1. Three-dimensional view of the proposed new variable coil structure.

Fig. 2. Diagram of EBs clipped in charging stands [16].

CC and CV by using two additional switches on the transmitter side to reconfigure the transmitter coil structure. This topology can achieve ZPA operation, fixed operating frequency, and zero-voltage switching (ZVS), which will lower the power rating of power switches and improve efficiency. Finally, a laboratory prototype with a charging current of 2 A and a charging voltage of 48 V is built to verify the proposed method.

Compared to the approach presented in [3], this topology is more compact due to the fact that only the series compensation is used on the receiver side, while [3] used an inductor, three capacitors, and two switches on the receiver side. Therefore, by only using series compensation will reduce the weight and save the installation space of the EB compared to [3]. Compared to [9], this proposed method uses fewer switches.

II. Theoretical Analysis

A. Proposed New Variable Coil Structure

The proposed new variable coil structure is shown Fig. 1. It can be seen that unipolar and bipolar coils are connected in series and are placed overlapped as the transmitter coil, where the bipolar coil is split into two coils, L_{T1} and L_{T2}, while the unipolar coil L_{T3} remains unchanged. On the receiver side, a unipolar coil L_S is adopted. Ferrites are used to enhance the magnetic coupling. According to [11], [12], and [15], the mutual inductance between the unipolar coil and bipolar coil is zero when they are overlapped. Therefore, there are only two mutual inductances in the proposed structure, i.e., the mutual inductance (M_1) between L_{T1} and L_{T2} and the mutual inductance (M_2) between the L_{T3} and L_S. For simplifying the analysis, the parasitic resistances of the coils are ignored.

It should be noted that the proposed coil structure is used for charging EBs. EBs are usually parked at public parking spots as shown in Fig. 2, so it is easy to align the transmitter coil at the charging station with the receiver coil at the EB. As a result, the mutual inductances will be easily fixed [3]. It is worth mentioning that the proposed idea is also valid for those applications where the receiver coil can be easily aligned with the transmitter coil. EBs are chosen as the targeted application because the EB is a very typical example to illustrate the proposed idea. Indeed, the proposed IPT system shows great potential in the EB market.

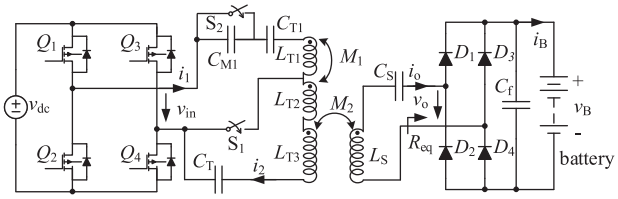

Fig. 3. Circuit topology of the proposed IPT system based on the new variable coil structure.

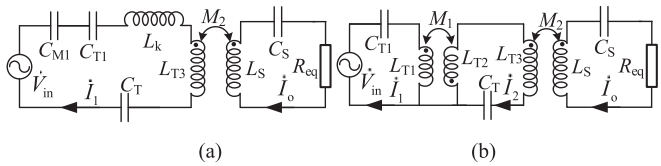

Fig. 4. Equivalent circuits of the proposed IPT system. (a) When S_1 and S_2 are turned OFF. (b) When S_1 and S_2 are turned ON.

B. Circuit Topology

The circuit topology of the proposed IPT system is shown in Fig. 3, where two additional switches S_1 and S_2 are used to reconfigure the transmitter circuit structure. The low-cost relay is used as the switch to select the charging mode because the switching time will not affect the performance of the whole charging system [10]. The output voltage of the inverter and the input voltage of the rectifier can be expressed as [3]

$$\begin{cases} V_{\text{in}} = 2\sqrt{2}V_{\text{dc}}/\pi \\ V_o = 2\sqrt{2}V_B/\pi \\ I_o = \pi\sqrt{2}I_B/4. \end{cases} \tag{1}$$

C_{T1}, C_{M1}, C_T, and C_S are the resonant capacitors for both sides. In order to tune the IPT system, the compensation capacitors can be calculated as

$$\begin{cases} C_{M1} = \left(\omega^2 M_1\right)^{-1} & C_T = \left[\omega^2\left(L_{T2}+L_{T3}\right)\right]^{-1} \\ C_{T1} = \left(\omega^2 L_{T1}\right)^{-1} & C_S = \left(\omega^2 L_S\right)^{-1}. \end{cases} \tag{2}$$

By turning ON/OFF the switches, two transmitter circuit structures can be obtained, leading to two operation modes of the proposed IPT system. The detailed analysis will be presented as follows.

C. Circuit Modeling in the CC Mode

When S_1 and S_2 are turned OFF, the equivalent circuit of the proposed system becomes the one shown in Fig. 4(a). R_{eq} is the equivalent resistance of the rectifier, i.e., $R_{\text{eq}} = 8R_L\left(\pi^2\right)^{-1}$ [12]. In this case, the coils L_{T1} and L_{T2} are connected in series

with the source. The equivalent inductor of the connection of L_{T1} and L_{T2} is denoted as L_k, which can be expressed as $L_{\rm k} = L_{T1} + L_{T2} + 2M_1$.

According to Kirchhoff's voltage law and mutual coupling theory, the relationships between the currents and the voltages on the transmitter side and the receiver side are given by

$$\begin{cases} \dot{V}_{\rm in} = \left[-jX_{CT1} - jX_{CM1} - jX_{CT} + jX_{LK} + jX_{T3}\right]\dot{I}_1 \\ \qquad\quad +jX_{M2}\dot{I}_o \\ 0 = -jX_{M2}\dot{I}_1 + \left(jX_{LS} + -jX_{CS} + R_{\rm eq}\right)\dot{I}_o \end{cases} \tag{3}$$

where

$$\begin{cases} X_{LK} = \omega\left(L_{T1} + L_{T2} + 2M_1\right) & X_{T3} = \omega L_{T3} \\ X_{CT1} = 1/\omega C_{T1} & X_{M2} = \omega M_2 \\ X_{CM1} = 1/\omega C_{M1} & X_{LS} = \omega L_S \\ X_{CT} = 1/\omega C_T & X_{CS} = 1/\omega C_S. \end{cases} \tag{4}$$

Substituting (2) and (4) into (3), the following equations can be obtained:

$$\begin{cases} \dot{I}_o = \dot{V}_{\rm in}/j\omega M_2 & \dot{V}_o = \dot{I}_o R_{\rm eq} = \dot{V}_{\rm in} R_{\rm eq}/j\omega M_2 \\ \dot{I}_1 = \dot{V}_{\rm in} R_{\rm eq}/\omega^2 M_2^2 & Z_{\rm in} = \dot{V}_{\rm in}/\dot{I}_1 = \omega^2 M_2^2/R_{\rm eq}. \end{cases} \tag{5}$$

It can be found from (5) that the output current I_o is independent of the load $R_{\rm eq}$. Specifically, I_o is only determined by the output voltage of the inverter $V_{\rm in}$, the operating frequency ω, and the mutual inductance M_2. With a constant input voltage, the output current can be considered as a CC source, provided that the operating frequency and mutual inductance are fixed. Since the input impedance of the IPT system is purely resistive, this IPT structure can achieve ZPA as well with fixed operating frequency.

D. Circuit Modeling in the CV Mode

When S_1 and S_2 are turned ON, the IPT system is changed from the CC mode to the CV mode, and the equivalent circuit of the IPT system is shown in Fig. 4(b). Similarly, the following equations can be obtained:

$$\begin{cases} \dot{V}_{\rm in} = \left[-jX_{CT1} + jX_{LT1}\right]\dot{I}_1 + jX_{M1}\dot{I}_2 \\ 0 = -jX_{M1}\dot{I}_1 + \left(jX_{LT2} - jX_{CT} + jX_{LT3}\right)\dot{I}_2 \\ \qquad +jX_{M2}\dot{I}_o \\ 0 = -jX_{M2}\dot{I}_2 + \left(jX_{LS} - jX_{CS} + R_{\rm eq}\right)\dot{I}_o \end{cases} \tag{6}$$

where

$$\begin{cases} X_{M1} = \omega M_1, \quad X_{LT2} = \omega L_{T2} \\ X_{LT1} = \omega L_{T1}. \end{cases} \tag{7}$$

Substituting (2), (4), and (7) into (6), the currents and voltages can be described as

$$\begin{cases} \dot{I}_o = \dot{V}_{\rm in} M_2/R_{\rm eq} M_1 & \dot{V}_o = \dot{I}_o R_{\rm eq} = \dot{V}_{\rm in} M_2/M_1 \\ \dot{I}_1 = \dot{V}_{\rm in} M_2^2/R_{\rm eq} M_1^2 & Z_{\rm in} = \dot{V}_{\rm in}/\dot{I}_1 = M_1^2/R_{\rm eq} M_2^2 \\ \dot{I}_2 = \dot{V}_{\rm in}/j\omega M_1. \end{cases} \tag{8}$$

TABLE I
SYSTEM SPECIFICATION AND PARAMETER VALUES

$V_{\rm dc}$	L_{T1}	L_{T2}	L_{T3}	L_S	M1
60 V	10.8 μH	12.96 μH	30.36 μH	39.87 μH	9.67 μH
M_2	C_{M1}	C_{T1}	C_T	C_S	f
7.73 μH	6.27 nF	9.83 nF	2.34 nF	2.56 nF	500 kHz

It is clear that the output voltage V_o is independent of the load, and it is only related to the output voltage of the inverter $V_{\rm in}$ and the mutual inductances M_1 and M_2. Besides, the input impedance is also purely resistive.

Therefore, the proposed IPT system can work either in the CC mode or the CV mode by flexibly switching into different transmitter coil structures, and both the two modes can achieve ZPA. Besides, the gyrator-based analysis method is another method that can be used to understand the CC and CV characteristics [17].

III. PARAMETER DESIGN

Substituting (1) into (5) and (8), the mutual inductances can be calculated as

$$\begin{cases} M_1 = 8V_{\rm dc}^2/\omega V_B I_B \pi^2 \\ M_2 = 8V_{\rm dc}/\omega I_B \pi^2. \end{cases} \tag{9}$$

In this letter, the input dc voltage is chosen as 60 V ($V_{\rm dc} =$ 60 A), and the operating frequency is 500 kHz. A charging current of 2 A ($I_B = 2$ A) and a charging voltage of 48 V ($V_B = 48$ A), which have been widely used for charging low-power EBs, are also adopted here. Then, the mutual inductances can be calculated as $\sim$9.67 and $\sim$7.74 μH according to (9).

Traditionally, the sizes of the coils can be adjusted according to the available installation space of various applications. Once the sizes of the coils are determined, the turns of the coils should be chosen to achieve the required mutual inductances. The FEA software Maxwell is usually used to design the proposed magnetic coils with the desired mutual inductances by varying the turns of the coils, which is given in detail in [12], [14], and [15].

The dimensions of the magnetic coils are shown in Fig. 1, as an example. The air gap is set to 50 mm. Litz wire of 0.04 mm/700 strands and PC40 ferrite core are used to construct the coils. Finally, the turns of L_{T1}, L_{T2}, L_{T3}, and L_S are, respectively, calculated as 4, 5, 13, and 13 to achieve the desired mutual inductances with the help of Maxwell.

IV. EXPERIMENTAL RESULTS

Fig. 5 shows the laboratory prototype. The experimental parameters are listed in Table I. The allowed rating voltage of the battery is $\sim$57.6 V, and the rating current of the battery is 6 A.

The performance of the proposed IPT system in the CC mode will be first examined. Fig. 6(a) shows waveforms of the inverter's output voltage/current and the charging current/voltage. It can be found in Fig. 6(a) that the charging current is maintained at 2 A, and the input impedance is purely resistive. Besides, the inverter can achieve ZVS in the CC mode, as shown

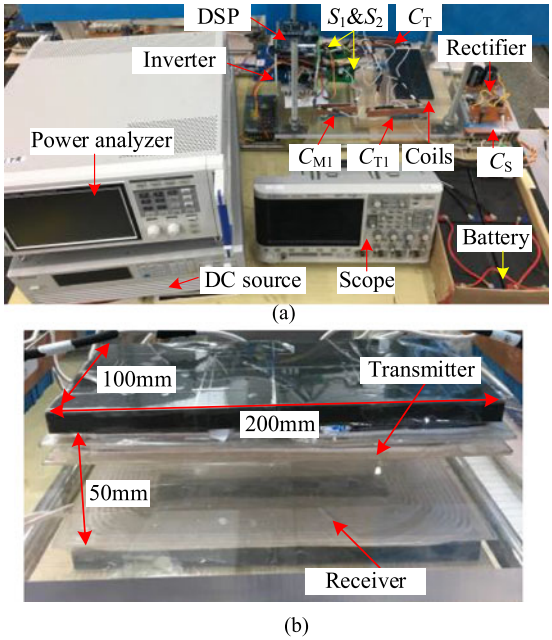

Fig. 5. Experimental setup. (a) Prototype of the proposed IPT system. (b) Coupling coils.

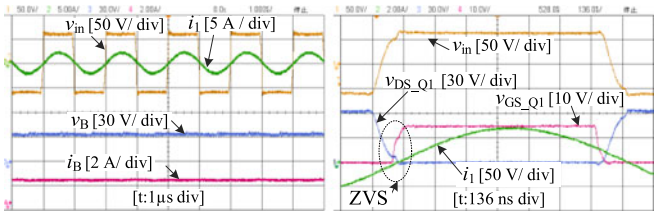

Fig. 6. Experimental waveforms in the CC mode. (a) Waveforms of v_{in}, i_1, v_B, and i_B. (b) Waveforms of Q_1.

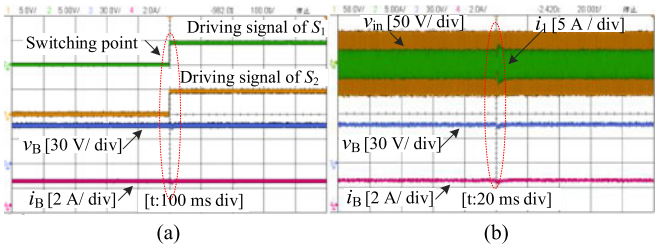

Fig. 7. Transient waveforms from the CC mode to the CV mode. (a) Waveforms of the driving signals of S_1 and S_2. (b) Waveforms of v_{in}, i_1, v_B, and i_B.

in Fig. 6(b). During the CC charging stage, the charging voltage will increase. Then, the charging mode will be changed into the CV mode when the charging voltage reaches 48 V.

Fig. 7 shows the transient waveforms from the CC mode to the CV mode. It demonstrates that the CC mode can be smoothly transferred to the CV mode by using the relay switches. The overall efficiency and power loss distribution are measured by a power analyzer in the switching point, as shown in Fig. 8. The overall efficiency (dc–dc) can reach as high as 91.014%, which is acceptable for the EB charging.

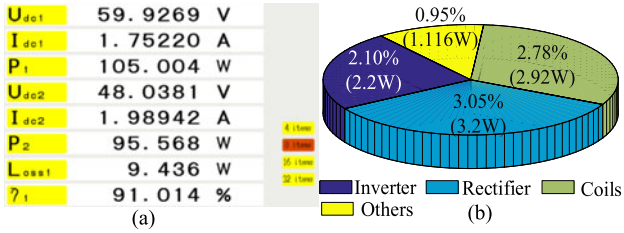

Fig. 8. Measured results. (a) Capture of power from the power analyzer. (b) Measured power loss distribution.

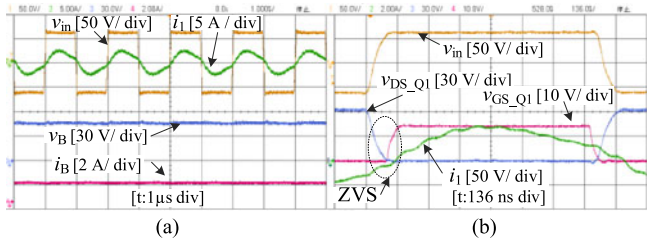

Fig. 9. Experimental waveforms in the CV mode. (a) Waveforms of v_{in}, i_1, v_B, and i_B. (b) Waveforms of Q_1.

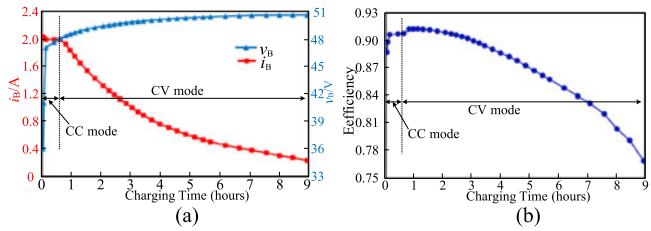

Fig. 10. Experimental results. (a) Measured charging profile. (b) Measured efficiencies.

Fig. 9 shows the corresponding waveforms in the CV mode. In this scenario, the IPT system can achieve ZPA and ZVS, simultaneously. The whole charging profile with charging current and charging voltage aginst charging time is depicted in Fig. 10(a), and the overall efficiencies aginst charging time is illustrated in Fig. 10(b). The voltage of the battery will be slightly increased during the charging process in the CV mode. The charging process will end up with the charging current decreasing to nearly zero.

V. Conclusion

A new-variable-coil-structure-based IPT system is proposed to charge EBs. By splitting and reconfiguring the transmitter coil structure, the proposed IPT system can achieve CC and CV outputs by switching between two circuit topologies. The proposed method is much simpler and more compact than the previous approaches. Furthermore, both CC and CV modes can realize ZPA and ZVS, simultaneously. The experimental results show the effectiveness of the proposed method, and the IPT system can achieve the overall efficiency as high as 91.014%, which is suitable for the EB applications.

REFERENCES

[1] H. Z. Z. Beh, G. A. Covic, and J. T. Boys, "Wireless fleet charging system for electric bicycles," *IEEE J. Emerg. Sel. Topics Power Electron.*, vol. 3, no. 1, pp. 75–86, Mar. 2015.

[2] H. Z. Z. Beh, G. A. Covic, and J. T. Boys, "Investigation of magnetic couplers in bicycle kickstands for wireless charging of electric bicycles," *IEEE J. Emerg. Sel. Topics Power Electron.*, vol. 3, no. 1, pp. 87–100, Mar. 2015.

[3] R. Mai, Y. Chen, Y. Li, Y. Zhang, G. Cao, and Z. He, "Inductive power transfer for massive electric bicycles charging based on hybrid topology switching with a single inverter," *IEEE Trans. Power Electron.*, vol. 32, no. 8, pp. 5897–5906, Aug. 2017.

[4] A. Khaligh and Z. Li, "Battery, ultracapacitor, fuel cell, and hybrid energy storage systems for electric, hybrid electric, fuel cell, and plug-in hybrid electric vehicles: State of the art," *IEEE Trans. Veh. Technol.*, vol. 59, no. 6, pp. 2806–2814, Jul. 2010.

[5] Y. Li, R. Mai, L. Lu, and Z. He, "Active and reactive currents decomposition based control of angle and magnitude of current for a parallel multiinverter IPT system," *IEEE Trans. Power Electron.*, vol. 32, no. 2, pp. 1602–1614, Feb. 2017.

[6] Y. L. Li, Y. Sun, and X. Dai, "μ-synthesis for frequency uncertainty of the ICPT system," *IEEE Trans. Ind. Electron.*, vol. 60, no. 1, pp. 291–300, Jan. 2013.

[7] C.-S. Wang, G. A. Covic, and O. H. Stielau, "Power transfer capability and bifurcation phenomena of loosely coupled inductive power transfer systems," *IEEE Trans. Ind. Electron.*, vol. 51, no. 1, pp. 148–157, Feb. 2004.

[8] W. Zhang, S. C. Wong, C. K. Tse, and Q. Chen, "Analysis and comparison of secondary series- and parallel-compensated inductive power transfer systems operating for optimal efficiency and load-independent voltage-transfer ratio," *IEEE Trans. Power Electron.*, vol. 29, no. 6, pp. 2979–2990, Jun. 2014.

[9] X. Qu, H. Han, S. C. Wong, C. K. Tse, and W. Chen, "Hybrid IPT topologies with constant current or constant voltage output for battery charging applications," *IEEE Trans. Power Electron.*, vol. 30, no. 11, pp. 6329–6337, Nov. 2015.

[10] W. Zhong and S. Y. R. Hui, "Reconfigurable wireless power transfer systems with high energy efficiency over wide load range," *IEEE Trans. Power Electron.*, to be published.

[11] M. Budhia, J. T. Boys, G. A. Covic, and C. Huang, "Development of a single-sided flux magnetic coupler for electric vehicle IPT charging systems," *IEEE Trans. Ind. Electron.*, vol. 60, no. 1, pp. 318–328, Jan. 2013.

[12] Y. Li, T. Lin, R. Mai, L. Huang, and Z. He, "Compact double-sided decoupled coils based WPT systems for high power applications: Analysis, design and experimental verification," *IEEE Trans. Transport. Electrific.*, vol. 4, no. 1, pp. 64–75, Mar. 2018.

[13] R. W. Erickson and D. Maksimovic, *Fundamentals of Power Electronics*, 2nd ed. Norwell, MA, USA: Kluwer, 2001.

[14] X. Qu, W. Zhang, S. C. Wong, and C. K. Tse, "Design of a current-source output inductive power transfer LED lighting system," *IEEE J. Emer. Sel. Topics Power Electron.*, vol. 3, no. 1, pp. 306–314, Mar. 2015.

[15] T. Kan, T. D. Nguyen, J. C. White, R. K. Malhan, and C. C. Mi, "A new integration method for an electric vehicle wireless charging system using LCC compensation topology: analysis and design," *IEEE Trans. Power Electron.*, vol. 32, no. 2, pp. 1638–1650, Feb. 2017.

[16] Alamy Stock. Row of for Hire BiciMad Electric Bikes in their Charging Stands, Madrid, Spain, Jun. 25, 2015. [Online]. Available: http://www.alamy.com/stock-photo-row-of-for-hire-bicimad-electric-bikes-in-their-charging-stands-madrid-83327187.htmlcompensation%20networks

[17] Y. H. Sohn, B. H. Choi, G.-H. Cho, and C. T. Rim, "Gyrator-based analysis of resonant circuits in inductive power transfer systems," *IEEE Trans. Power Electron.*, vol. 31, no. 10, pp. 6824–6843, Oct. 2016.